Available online at www.sciencedirect.com
SCIENCE DIRECT®
Journal of Chromatography A, 1034 (2004) 55–68
JOURNAL OF CHROMATOGRAPHY A
www.elsevier.com/locate/chroma

Charge regulation in protein ion-exchange chromatography: Development and experimental evaluation of a theory based on hydrogen ion Donnan equilibrium

Hong Shen, Douglas D. Frey*

Department of Chemical and Biochemical Engineering, University of Maryland Baltimore County, 1000 Hilltop Circle, Baltimore, MD 21250, USA

Received 30 September 2003; received in revised form 27 January 2004; accepted 27 January 2004

Abstract

An extension of the stoichiometric displacement (SD) model for the ion-exchange adsorption of dilute proteins is developed which accounts for the effects of hydrogen ion Donnan equilibrium on the protein charge. The ability of the new model to fit retention data when the fluid phase pH is near the protein p*I* and the effects of hydrogen ion Donnan equilibrium are important is examined using four different proteins and four different column packings. The results indicate that the model is able to fit retention data using values for the protein p*I* and the change in protein charge with pH at the p*I*, i.e., $(dz/dpH)_{pI}$, that are significantly closer to the values of these parameters determined by isoelectric focusing and acid–base titrametry in free solution, respectively, as compared to the values obtained by determining the characteristic binding change as a function of pH using the traditional stoichiometric displacement model. This suggests that when the fluid phase pH is near the protein p*I*, charge regulation is an important cause of the discrepancy between the electrical charge of a protein in free solution and the characteristic binding charge from the stoichiometric displacement model. The results also indicate that for the case where the fluid phase pH is near the protein p*I*, the new model accounts for the effect of charge regulation during protein ion-exchange adsorption more accurately than previous models in the literature.

Keywords: Stoichiometric displacement model; Ion-exchange equilibrium; Proteins

1. Introduction

The net charge on a polyelectrolyte depends not only on the pH and ionic strength of the surrounding fluid, but also on the proximity of the polyelectrolyte to other charged surfaces. The last effect, which is generally termed "charge regulation," results from electrostatic interactions between the charged surface and the ionogenic functional groups on the polyelectrolyte [1–5]. Although many models of protein ion-exchange equilibrium have been described in the literature [6–11], only the models of Sluyterman and Elgersma [12] and Ståhlberg and Jönsson [13] account specifically for the change in the protein charge caused by electrostatic interactions with the adsorbent surface. The scarcity of previous efforts to theoretically model this case is surprising since a number of references have discussed the importance of the change in protein charge caused by adsorption during ion-exchange chromatography [8,14,15]. In addition, it has been reported that the optimal resolution between two proteins when using ion-exchange chromatography with salt gradient elution is often achieved when the fluid phase pH is near the protein p*I* [16]. The effects of the change in protein charge caused by adsorption are likely to be particularly important under these conditions since the relative change in protein net charge is largest when the fluid phase pH and the protein p*I* are similar in value. Furthermore, when a pH gradient is used for eluting proteins in ion-exchange chromatography, such as in the technique of chromatofocusing, accounting for the change in protein charge caused by adsorption may also be important since proteins generally elute near their p*I* in these types of processes.

Two basic approaches are possible to account for the change in protein charge caused by adsorption onto a charged surface. As described by Ståhlberg and Jönsson [13], one approach consists of using a colloidal model based on a microscopic description where the adsorbed phase is represented as an electrical double layer, and the Poisson–Boltzmann equation is then used to describe the electrostatic

* Corresponding author. Tel.: +1-410-455-3418; fax: +1-410-455-6500.
E-mail address: dfrey1@umbc.edu (D.D. Frey).

0021-9673/$ – see front matter © 2004 Elsevier B.V. All rights reserved.
doi:10.1016/j.chroma.2004.01.039

effect produced by the adsorbent on the standard free energy of dissociation of the ionogenic groups on the protein. This first approach can also be interpreted as using the local pH in the electrical double layer determined employing a Boltzmann distribution for the hydrogen ions, as opposed to using the pH in the bulk fluid, for the purpose of calculating the degree of dissociation of an ionogenic group on the protein. The second basic approach is illustrated by the model of Sluyterman and Elgersma [12] and consists of using a non-colloidal model where the adsorbed phase is visualized as being uniform in composition, and the macroscopic laws of thermodynamics are then applied so that changes in protein charge due to adsorption are accounting for using the pH difference between the adsorbed and fluid phases caused by hydrogen ion Donnan equilibrium.

Although the models developed by Ståhlberg and Jönsson [13] and Sluyterman and Elgersma [12] are reasonable descriptions of charge regulation during protein ion-exchange adsorption, the specific results obtained by these workers have limited uses in practice. In particular, the analytical approximation developed by Ståhlberg and Jönsson does not apply to the case of most interest when considering protein charge regulation, which is the case when the fluid phase pH is near the protein p*I*. Similarly, although the analytical result of Sluyterman and Elgersma does apply to this case and is algebraically simple, it is limited in accuracy when fitting experimental data, as shown later.

The purpose of the present study is to develop a model describing charge regulation for the ion-exchange adsorption of a dilute protein which is simple enough for routine use in data fitting and chromatographic process design, but which nevertheless describes the phenomena involved with reasonable accuracy. To achieve this, a non-colloidal, macroscopic model will be employed which is related to the model of Sluyterman and Elgersma [12], but where the most restrictive assumptions employed by Sluyterman and Elgersma are eliminated. Although, as an alternative, an improved version of the colloidal model of Ståhlberg and Jönsson [13] could also be developed, in practice colloidal models tend to be prohibitively complex for routine use. Furthermore, as shown by Overbeek [17], non-colloidal models for the adsorption of ions onto a charged surface represent the corresponding colloidal model asymptotically in the limit where the dimensionless potential energy of the adsorbed ion on the surface (i.e., $zF\psi_s/RT$) becomes small compared to unity. This asymptotic relationship tends to ensure that non-colloidal models of protein charge regulation, if properly formulated, will represent the actual behavior with acceptable accuracy, particularly for the case considered here where the pH is near the protein p*I* and the protein net charge (i.e., z) is not large.

In addition to developing a model that accounts for the change in protein charge during ion-exchange adsorption, another goal of the present study is to test experimentally the new model developed here, the model of Sluyterman and Elgersma [12], the model of Ståhlberg and Jönsson [13], and the widely used stoichiometric displacement (SD) model [6] for the case where the fluid phase pH is near the protein p*I*. Although there are many data reported for the isocratic elution of proteins in ion-exchange chromatography [7,8,11,18–20], these data are usually obtained over a large pH range of much more than one pH unit so that only a limited amount of data exists near the protein p*I* where the effects of charge regulation are likely to be important. In addition, due to the fact that a broad pH range was utilized, many previous studies have employed a different buffering species in different pH ranges which, according to some investigators, can influence the adsorption equilibrium behavior [21]. In the present study, one set of experiments utilizing only one buffering species will be carried out for each combination of protein and column packing, and all the data will be obtained in a narrow pH interval near the protein p*I*, which should facilitate comparisons between data and theory for the case of interest here where the pH and protein p*I* are close in value.

2. Theory

2.1. Stoichiometic displacement model

The most widely used model for protein ion-exchange adsorption is the stoichiometric displacement model, which is based on the application of mass-action equilibrium to an adsorbed phase that is assumed uniform in composition [6]. Although the SD model is relatively simple and does not account for protein charge regulation, it is nevertheless a useful base case to which more complex models can be compared. For the case of a dilute protein adsorbing onto an anion exchanger with the chloride ion as the counterion, the SD model leads to:

$$K_d = K_B \left(\frac{q_{Cl^-}}{C_{Cl^-}} \right)^z \tag{1}$$

where the distribution coefficient, K_d, is defined to be the ratio of the protein concentration in the adsorbed and fluid phases, q_{Cl^-} is the chloride ion concentration in the adsorbed phase, which is equivalent to the concentration of ion-exchange functional groups in the adsorbent if the protein is dilute, and K_B is a constant.

2.2. Model of Sluyterman and Elgersma

As mentioned above, one model which makes an attempt—albeit highly simplified—to account for charge regulation during protein ion-exchange adsorption is the model developed by Sluyterman and Elgersma [12]. The starting point for this model is to visualize the protein as potentially existing in the three charge states +1, 0, and −1, as described by the two acid–base equilibrium constants K_1 and K_2. Since for this case the protein isoelectric point is given by the average of pK_1 and pK_2, and incorporating

an expression for hydrogen ion Donnan equilibrium, the following relation can be developed for the case where the uncharged protein has a distribution coefficient of unity:

$$\mathrm{p}I' - \mathrm{p}I = -\frac{\phi}{4.6} \tag{2}$$

In Eq. (2), pI is the isoelectric point of the protein, pI' is the pH where the distribution coefficient accounting for all three charged forms of the protein is unity, and ϕ is the dimensionless Donnan potential as defined in Section 2.4.2. After first developing Eq. (2), Sluyterman and Elgersma next appear to abandon the depiction of the protein as exhibiting three charge states by using the follow relation based on the Boltzmann distribution which assumes that the protein has a single charge state and is distributed between two phases of uniform, but different, electric potential:

$$\ln(K_\mathrm{d}) = -\phi z \tag{3}$$

In Eq. (3), K_d is the distribution coefficient and z is the charge on the protein. If it is further assumed that the protein charge is a linear function of pH, then Eq. (3) leads to

$$\ln(K_\mathrm{d}) = -\phi \frac{\mathrm{d}z}{\mathrm{dpH}}(\mathrm{pH} - \mathrm{p}I') \tag{4}$$

Combining Eqs. (2) and (4) to eliminate pI' leads to the main result of Sluyterman and Elgersma [12], which can be written as:

$$\ln(K_\mathrm{d}) = -\phi \left(\frac{\mathrm{d}z}{\mathrm{dpH}}\right)\left[(\mathrm{pH} - \mathrm{p}I) + \frac{\phi}{4.6}\right] \tag{5}$$

In the final expression developed by Sluyterman and Elgersma, the pH in Eq. (5) was interpreted to be the apparent isoelectric point observed in chromatofocusing, denoted as pI_app, due to the fact that in chromatofocusing the protein travels through the column at a fixed pH and fluid phase composition. Furthermore, for the case of chromatofocusing the distribution coefficient, K_d, can be equated to the ratio of the buffering capacities in the adsorbed and fluid phases, which is a function of pH, to arrive at a final expression which relates the apparent isoelectric point to properties of the protein, column packing, and fluid phase.

Although Eq. (5) is a simple means to represent protein adsorption equilibrium, the derivation just given illustrates several of its deficiencies. In particular, it does not account for the change in the distribution among the charge states of a protein upon adsorption. It also assumes the distribution coefficient for an uncharged protein is unity, so that it does not account properly for nonelectrostatic contributions to adsorption, such as the contribution of hydrophobic interactions. In addition, it does not account for a nonlinear relation between the protein charge and pH. Finally, since each ionizable functional group on the protein is titrated in a range of approximately one pH unit, the use in the model of just three charge states implies that when $(\mathrm{d}z/\mathrm{dpH})_{\mathrm{p}I} \geq 3$ the model is being extrapolated into a range where the corresponding values for K_1 and K_2 are not positive real numbers. In the sections that follow, it will be shown that a more rigorous theory that accounts for these effects can be developed and used to fit experimental data more consistently than Eq. (5).

2.3. Model of Ståhlberg and Jönsson

To account for charge regulation during protein ion-exchange adsorption, Ståhlberg and Jönsson [13] employed a colloidal model in which the adsorbed phase is represented as an electrical double layer, and the linearized Poisson–Boltzmann equation is used to describe the electrostatic interactions between the protein and the adsorbent surface. To simplify the mathematical development, the protein and the adsorbent surface were represented as flat charged plates oriented parallel to each other, and the charge densities of the surfaces representing both the protein and the adsorbent were assumed to depend on the electric potential at those surfaces. For the case where the charge density on the adsorbent surface is larger than that on the protein surface, the minimum free energy of the system when the distance between the protein and surface is varied was shown to be

$$\frac{\Delta G_\mathrm{m}}{A_\mathrm{P}} = \frac{\sigma_\mathrm{P}^2}{\kappa\varepsilon_0\varepsilon_\mathrm{r}(1-B)} \tag{6}$$

where σ_p is the charge density on the protein surface in the bulk fluid and B is given by

$$B = \frac{2F^2}{\kappa\varepsilon_0\varepsilon_\mathrm{r}A_\mathrm{P}^0 RT\ln(10)}\frac{\mathrm{d}z}{\mathrm{dpH}} \tag{7}$$

If the free energy minimum given by Eq. (6) is used to evaluate the distribution coefficient, the result can be written as

$$\begin{aligned}\ln k' &= \frac{\sigma_\mathrm{P}^2 A_\mathrm{P}}{F(2RT\varepsilon_0\varepsilon_\mathrm{r})^{1/2}(1-B)}\frac{1}{\sqrt{I}} + \ln(P) \\ &= \frac{135z^2}{(1-B)A_\mathrm{P}^0}\frac{1}{\sqrt{I}} + \ln(P)\end{aligned} \tag{8}$$

where k' is the retention factor, P is the phase ratio, and z is the net charge on the protein in the bulk fluid. In Eq. (8), the second equality results from substituting numerical values for the physical constants appearing on the right side of the first equality, and from assuming that the protein surface area interacting with the adsorbent is one half the total protein surface area.

Although the model of Ståhlberg and Jönsson [13] accounts for protein charge regulation in a consistent manner, it is apparent that Eq. (8) cannot be used to predict the amount adsorbed when the protein in the bulk fluid is uncharged, i.e., when $z = 0$. Since the adsorption of proteins onto an ion-exchange adsorbent when the protein is uncharged in the bulk fluid is commonly observed in practice [7], this implies that, as noted by Ståhlberg and Jönsson, the above model does not adequately describe protein adsorption when the fluid phase pH is near the protein pI. Furthermore, even

when the full numerical result of Ståhlberg and Jönsson is used, the case where the fluid phase pH is near the protein p*I* can only be accounted for when the charge density on the adsorbent surface is small due to limitations in the linearized form of the Poisson–Boltzmann equation used in the model.

2.4. New theory for protein charge regulation based on hydrogen ion Donnan equilibrium

2.4.1. General considerations

In the theory presented here, the adsorbed phase, which is defined to be the phase containing the adsorbed eluites, is envisioned as being uniform in composition and electrical potential and as being three-dimensional, with one of the three dimensions being very thin. Since many column packings consist of an inert base material onto which the functional groups responsible for adsorption are chemically bonded, the adsorbed phase will generally constitute only a fraction of the total solid material in the column. To describe the electrostatic interactions between the protein and the column packing, the protein is represented as a dilute polyelectrolyte which behaves like a point charge as it distributes between the fluid and adsorbed phases. The description of the electrostatic interactions used here is therefore equivalent to that used by Albertsson [22] and Haynes et al. [23] to describe the partitioning of a protein between two immiscible aqueous liquid phases, and by Sassi et al. [24] to describe the partitioning of a protein between an aqueous liquid phase and a charged hydrogel, except that these previous studies did not account for hydrogen ion Donnan equilibrium. Each ionogenic group on the protein is assumed to ionize according to an acid–base equilibrium constant that remains fixed and independent of the total protein charge so that the proportions of the protein that exist in the various possible charged forms can be determined by extending the Henderson–Hasselbalch equation [25] to the case of a molecule with several ionogenic groups.

In representing phase equilibrium, it is assumed that the electrochemical potential difference between two phases for each charged form (or, equivalently, the Boltzmann distribution of each charge form between regions of different electrical potential) can be written in terms of the concentration and electrical potential energy of each charged form in the two phases, analogous to how these quantities would be written for a mixture of chemically distinct species [22–24]. It is also assumed that the species constituting the buffer and eluting salt do not bind specifically to the protein, or at least that the number of bound ions is fixed and not a function of pH or ionic strength, so that the protein net charge is completely determined by the pH in its local environment and the properties of the ionizable groups on the protein. In general, the binding of small ions to proteins is minimal near the protein isoelectric point [18,26], which is the region of primary interest in the present study, so that the assumption of negligible small ion binding is expected to be a reasonable approximation.

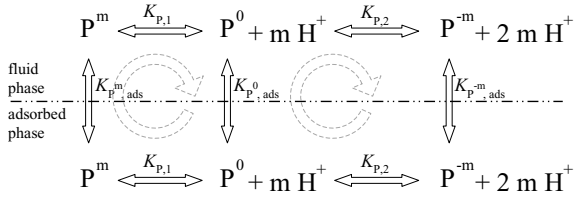

Fig. 1. Illustration of the multiple charge-state model for protein ion-exchange equilibrium. The dotted arrow denotes a closed equilibrium loop between neighboring protein charge forms.

Although in the visualization just described the polyelectrolyte under consideration, and hence its properties such as the p*I*, and the change in average charge with pH at the p*I*, $(dz/dpH)_{pI}$, correspond to the entire protein, an alternative interpretation can also be given that the polyelectrolyte under consideration corresponds to a specific charged region on the surface of the protein that is responsible for adsorption.

2.4.2. Multiple charge-state model

In order to develop a model where the protein can have any arbitrary charge, but where for mathematical simplicity there are only three charged forms to account for, an approximate *n* charge-state model will be introduced where the three representative charged states are presumed to be $-m$, 0, and m, which are the maximum negative charge state, the uncharged state, and maximum positive charge state of the protein, respectively, as illustrated in Fig. 1. It follows that the total number of charged states, n, is related to m by the relation $n = 2m + 1$. Although a selection of charged forms symmetrically distributed around the uncharged form is assumed, the following relations can also be extended to the case where this is not true.

To simplify the mathematical development, it is assumed that the protein isoelectric point is the same in the fluid and adsorbed phases, and correspondingly it is assumed that the equilibrium constant for the acid–base reaction for a particular pair of charged states shown in Fig. 1 is also the same in these two phases. Acid–base equilibrium for the $-m$, 0, and m charged states in the liquid phase can be written using these constants as:

$$K_{P,1} = \frac{C_{H^+}^m C_{P^0}}{C_{P^m}} \tag{9}$$

$$K_{P,2} = \frac{C_{H^+}^m C_{P^{-m}}}{C_{P^0}} \tag{10}$$

with an equivalent set of expressions applying to the adsorbed-phase acid–base equilibrium. The concentration of the $-m$, 0, and m charged forms in the fluid phase, assuming these are the only forms that exist, can be expressed according to the following extensions to the Henderson–Hasselbalch equations based on Eqs. (9) and (10):

$$C_{P^m} = \frac{C_P C_{H^+}^{2m}}{C_{H^+}^{2m} + K_{P,1} C_{H^+}^m + K_{P,1} K_{P,2}} \tag{11}$$

$$C_{P^0} = \frac{C_P K_{P,1} C_{H^+}^m}{C_{H^+}^{2m} + K_{P,1} C_{H^+}^m + K_{P,1} K_{P,2}} \quad (12)$$

$$C_{P^{-m}} = \frac{C_P K_{P,1} K_{P,2}}{C_{H^+}^{2m} + K_{P,1} C_{H^+}^m + K_{P,1} K_{P,2}} \quad (13)$$

where $C_P = C_{P^m} + C_{P^0} + C_{P^{-m}}$.

The reasonableness of using the model shown in Fig. 1 to represent the protein charge follows from the fact that Eqs. (11)–(13) yield an average charge for the protein in close agreement to the average charge determined from rigorously accounting for acid–base equilibrium between all of the possible n charged forms if the dissociation constants for the n charged forms are not too dissimilar, and if $K_{P,1}$ is equated to the product of the dissociation constants involving the $m-1$ negatively charged forms of the protein, and $K_{P,2}$ is equated to the product of the dissociation constants involving the $m-1$ positively charged forms of the protein. However, if the dissociation constants for all the n charged forms of the protein are assumed to be similar in value, it follows that the relations given in this section only apply accurately in a narrow pH region near the protein pI.

By using Eqs. (11)–(13), the pI and the value of $(dz/dpH)_{pI}$ for the protein can be expressed in terms of $K_{P,1}$ and $K_{P,2}$ as follows:

$$pI = -\frac{\ln(K_{P,1} K_{P,2})}{2m \ln(10)} \quad (14)$$

$$\left(\frac{dz}{dpH}\right)_{pI} = -\frac{2\ln(10)m^2}{\sqrt{K_{P,1}/K_{P,2}} + 2} \quad (15)$$

Solving Eqs. (14) and (15) for $K_{P,1}$ and $K_{P,2}$ yields:

$$K_{P,1} = -2 \times 10^{-m\,pI}\left[\frac{m^2 \ln(10)}{(dz/dpH)_{pI}} + 1\right] \quad (16)$$

$$K_{P,2} = -\frac{10^{-m\,pI}(dz/dpH)_{pI}}{2\left[m^2 \ln(10) + (dz/dpH)_{pI}\right]} \quad (17)$$

According to Overbeek [17] and Newman [27], the chemical potentials of an electrically neutral combination of ions in two phases in equilibrium are equal. Consequently, for the case of a protein adsorbing onto an anion-exchange adsorbent where Cl^- and Na^+ are the counterion and co-ion, respectively, adsorption equilibrium can be expressed using the following relations, which are extensions of relations used by Strong and Frey [28] for the case of a protein having a single charge state:

$$q_{P^m}^* q_{H^+}^{*-m} = K_{P^m,ads} C_{P^m} C_{H^+}^{-m} \quad (18)$$

$$q_{P^0}^* = K_{P^0,ads} C_{P^0} \quad (19)$$

$$q_{P^{-m}}^* q_{H^+}^{*m} = K_{P^{-m},ads} C_{P^{-m}} C_{H^+}^m \quad (20)$$

$$q_{Cl^-}^* q_{H^+}^* = K_{Cl^-,ads} C_{Cl^-} C_{H^+} \quad (21)$$

$$q_{Na^+}^* q_{H^+}^{-1} = K_{Na^+,ads} C_{Na^+} C_{H^+}^{-1} \quad (22)$$

In Eqs. (18)–(22), the superscript $*$ denotes an equilibrium value and $K_{i,ads}$ represents the interphase adsorption equilibrium constant which accounts for nonelectrostatic phenomena such as hydrophobic interactions, size exclusion effects, and osmostic pressure effects [17,24].

If the general equilibrium relations for protein adsorption are considered as shown in Fig. 1, it can be seen that since the acid–base dissociation constants $K_{P,1}$ and $K_{P,2}$ are assumed to be the same in the fluid and adsorbed phases, it follows that the adsorption equilibrium constants for the three charged forms as expressed in Eqs. (18)–(20) are also equal and can be represented by the single constant $K_{P,ads}$, i.e., $K_{P^{-m},ads} = K_{P^0,ads} = K_{P^m,ads} \equiv K_{P,ads}$. This assumption also leads to the conclusion that the three charged forms of the protein would have the same distribution coefficients if the adsorbent was uncharged and $q_{H^+}^* = C_{H^+}$. Although this assumption is convenient in order to simplify the mathematics, it may not always accurately represent the actual behavior since certain nonelectrostatic interactions, such as hydrophobic interactions, may depend on the protein charge state. Note finally that the electrically neutral ion combinations in Eqs. (18)–(22) are formed using the H^+ ion, and that Eq. (22) accounts for Donnan uptake of co-ion into the adsorbed phase, which may become a factor at high salt concentrations.

For convenience when fitting experimental data it is useful to develop a functional relation between the Donnan potential and the pH by assuming the existence of a single ionogenic functional group on the column packing having a dissociation constant of K_R. Acid–base equilibrium involving this group can then be expressed as:

$$q_{R^+} = \frac{q_{H^+} q_R}{K_R + q_{H^+}} \quad (23)$$

where q_R and q_{R^+} are the total concentration of the functional group and the concentration of the charged form of the functional group, respectively.

If the concentrations of the H^+ and OH^- ions in the adsorbed phase are assumed to be small, then the electroneutrality condition in that phase including the effect of co-ion uptake can be expressed as:

$$q_{R^+} + q_{Na^+} - q_{Cl^-} = 0 \quad (24)$$

If, in addition, the hydrogen ion is taken as the so-called "potential determining ion" so that the dimensionless Donnan potential, ϕ, can be identified with the quasi-electrostatic potential described by Sassi et al. [24] and Newman [27], then ϕ can be equated to $(\ln(C_{H^+}/q_{H^+}))$, and Eqs. (21)–(24) yield:

$$C_{Cl^-} K_{Cl^-,ads} \exp(\phi) - \frac{C_{Na^+} K_{Na^+,ads}}{\exp(\phi)} = \frac{C_{H^+} q_R}{K_R \exp(\phi) + C_{H^+}} \quad (25)$$

Eq. (25) is a cubic equation for the Donnan potential, and can be solved either analytically or numerically for this quantity. If either $K_{Na^+,ads} = 0$ (i.e., Donnan uptake of co-ion is ab-

sent) or if pK_R is large (i.e., the column packing is a strong-base ion exchanger), then Eq. (25) is a quadratic equation which can be solved explicitly for the Donnan potential.

If the Donnan potential is incorporated into Eqs. (18)–(20), the concentration of each charged form of the protein in the adsorbed phase can be further expressed as:

$$q^*_{p^m} = K_{P,ads} C_{P^m} \exp(\phi)^{-m} \quad (26)$$

$$q^*_{p^0} = K_{P,ads} C_{P^0} \quad (27)$$

$$q^*_{p^{-m}} = K_{P,ads} C_{P^{-m}} \exp(\phi)^{m} \quad (28)$$

It can be seen that the preceding development is equivalent to assuming a Boltzmann distribution for each charged form using the Donnan potential to define the energy states.

For the case of a protein having multiple charged forms, the distribution coefficient, K_d, is defined as the ratio of the total of the individual protein forms in the adsorbed phase per unit volume of that phase to the same quantity in the fluid phase. Consequently, by combining Eqs. (11)–(13) and (26)–(28), K_d can be expressed as:

$$K_d = K_{P,ads} \exp(m\phi) \left[\frac{(dz/dpH)_{pI}(1 - 10^{m(pI-pH)} \exp(-m\phi))^2 - 2\ln(10)m^2 10^{m(pI-pH)} \exp(-m\phi)}{(dz/dpH)_{pI}(1 - 10^{m(pI-pH)})^2 - 2\ln(10)m^2 10^{m(pI-pH)}} \right] \quad (29)$$

Eq. (29) can also be solved explicitly for the fluid phase pH, although the final form of the solution is too lengthy to be reported here. Nevertheless, this alternative form of Eq. (29) can be applied to chromatofocusing in a manner similar to Eq. (5). Although Eq. (29) was developed assuming that m is an integer, when fitting experimental data it is convenient to allow m to have non-integer values. In cases where m is a non-integer number it will nevertheless be assumed that the number of charge states between $-m$ and m is still given by $2m + 1$, and consequently n may also be a non-integer number.

When applying Eq. (29) it is useful to recognize several aspects of that equation. One aspect is that K_d approaches a finite limit as the fluid phase pH becomes large so that a single charged form exists in both the fluid and adsorbed phases, i.e.,

$$\lim_{pH\to\infty} (K_d) = K_{p,ads} \exp(m\phi) = \frac{K_{p,ads}}{K^m_{Cl^-,ads}} \left(\frac{q_{Cl^-}}{C_{Cl^-}} \right)^m \quad (30)$$

where the second equality follows from Eq. (21) and the term on the far right side of Eq. (30) has the same form as the SD model discussed previously. Furthermore, by comparing Eq. (29) and first equality in Eq. (30), it follows that Eq. (29) is an extension of the SD model to the case where hydrogen ion Donnan equilibrium affects the protein charge, with the quantity in square brackets in Eq. (29) being the factor which corrects the SD model for this effect. Another aspect of Eq. (29) is that the maximum absolute value of $(dz/dpH)_{pI}$ for a given value of m results when $K_{P,1} = K_{P,2}$, as can be seen from Eq. (15), in which case this maximum value is given by $-2\ m^2 \ln(10)/3$.

A final aspect of Eq. (29), as well as Eq. (25), is that the activity coefficients which account for thermodynamically nonideal behavior are incorporated into the interphase adsorption equilibrium constants. This implies that the pH in Eq. (29) is given by $-\log(C_{H^+})$, whereas pH values measured using a standard pH electrode are equivalent to $-\log(a_{H^+})$, where a_{H^+} is the activity of the hydrogen ion. These two quantities differ by the amount $-\log(\gamma_{H^+})$, where γ_{H^+} is the activity coefficient of the hydrogen ion. According to Newman [27], γ_{H^+} varies from a minimum of 0.8 at an ionic strength of 0.25 M to unity at ionic strengths of 0 and 2 M. The average deviation between the values of $-\log(C_{H^+})$ and $-\log(a_{H^+})$ in the range of ionic strengths employed in the present study is therefore expected to be approximately $-\log(0.9)$ or 0.1, which is also expected to be the approximate error in the pI values determined by fitting Eq. (29) to experimental data if $-\log(a_{H^+})$ is used for the pH in that equation. Use of pH values measured with a pH electrode in Eq. (29) is therefore considered to be an acceptable approximation in the present study.

2.4.3. Relation between equilibrium parameters and eluite transit times

According to a material balance, the transit time for a retained eluite can be expressed as follows [29]:

$$t = \left(\frac{L}{v_{fluid}} \right) \left[1 + \frac{(1-\alpha)}{\alpha} \varepsilon + f \frac{(1-\alpha)(1-\varepsilon)}{\alpha} K_d \right] \quad (31)$$

where L is the column length, v_{fluid} is the linear fluid velocity, α and ε are the interparticle and intraparticle void volumes, respectively, and K_d is the equilibrium mass of protein adsorbed per unit volume of the actual adsorbed phase divided by the concentration of protein in the fluid phase. The parameter f in Eq. (31) accounts for the fact that the adsorbed phase occupies only a fraction of the entire solid material constituting the column packing. The need for this parameter results from the fact that certain other parameters used in the relations in the previous section, such as the hydrogen ion concentration in the adsorbed phase used in Eqs. (18)–(22), need to reflect the true concentration of a species, as opposed to the mass of that species per unit volume of the total solid material or per unit volume of column. For example, if the quantity of functional groups R per unit volume of column, $q_{R,col}$, is known, then the quantity of these functional groups per unit volume of adsorbed phase, q_R, as used in Eq. (23) is given by:

$$q_R = \frac{4 q_{R,col}}{\pi D^2 L f (1-\alpha)(1-\varepsilon)} \quad (32)$$

The time t_0 is defined to be the time needed for an unretained eluite to travel through the column, and for ion-exchange chromatography this quantity is usually determined at high

salt concentrations. In practice, however, it may be difficult, or even impossible, to select a salt concentration to ensure that K_d is identically zero due to the presence of hydrophobic interactions between the protein and column packing at high salt concentrations. In addition, even if hydrophobic interactions are assumed absent, the fact that Donnan uptake of co-ion into the adsorbed phase as described by Eq. (22) is included in the model used here implies that a non-zero value for K_d is predicted theoretically as the salt concentration becomes large. Consequently, a reasonably high salt concentration can be selected to determine a working value of t_0 which corresponds to a presumably small distribution coefficient, denoted here as $K_{d,hs}$. The relation between t_0 and $K_{d,hs}$ then becomes:

$$t_0 = \left(\frac{L}{v_{fluid}}\right)\left[1 + \frac{(1-\alpha)}{\alpha}\varepsilon + f\frac{(1-\alpha)(1-\varepsilon)}{\alpha}K_{d,hs}\right] \quad (33)$$

where $t_0 = t_M - t_D$, t_M is the measured transit time under high salt conditions and t_D is the time associated with the extra-column volume. In cases where $K_{d,hs}$ and the interparticle void volume, α, are known or can be reliably estimated, Eq. (33) can be used to determine the intraparticle void volume, ε, from measurements of t_0.

The retention factor k' is defined as:

$$k' = \frac{t - t_0}{t_0} \quad (34)$$

where t is the measured transit time of a retained eluite corrected for the extra-column volume. Eqs. (31), (33) and (34) can be combined to yield:

$$k' = \frac{f(1-\alpha)(1-\varepsilon)(K_d - K_{d,hs})}{\alpha(1 - fK_{d,hs}) + (1-\alpha)\varepsilon(1 - fK_{d,hs}) + fK_{d,hs}} \quad (35)$$

For the case where $f = 1$ and $K_{d,hs} = 0$, Eq. (35) reduces to:

$$k' = \frac{(1-\alpha)(1-\varepsilon)K_d}{\alpha + (1-\alpha)\varepsilon} = PK_d \quad (36)$$

Although for the sake of completeness the parameter $K_{d,hs}$ has been introduced into the above equations, and although this parameter is expected to be non-zero in certain cases, for the particular cases investigated in the present study it was determined that good agreement between experimental data and predictions from Eq. (29) could be obtained with this parameter neglected.

3. Experimental methods

3.1. Materials and columns

Myoglobin from horse heart and β-lactoglobulin A from bovine milk were products M 1882 and M 7880 obtained from Sigma (St. Louis, MO, USA). Triethanolamine, trisma base, NaCl and HCl were also obtained from Sigma, and 1-methylpiperzaine and 1,4-dimethylpiperazine were obtained from Aldrich (Milwaukee, WI, USA). All buffer solutions were prepared using distilled water and were degassed by vacuum filtering using a 47 mm diameter nylon membrane filter with 0.2 μm pores (Whatman, Clifton, NJ, USA). Each injection sample was dissolved into the elution buffer and filtered with a PVDF syringe driven filter with 0.22 μm pore size (Millipore, Bedford, MA, USA).

The columns used were a 5 × 0.5 cm i.d. Mono Q HR 5/5 strong-base anion-exchange column and a 5 × 0.5 cm i.d. Mono P HR 5/5 weak-base anion-exchange column, both obtained from Amersham Biosciences (Piscataway, NJ, USA). According to the manufacturer, the ionic capacity of these two columns are 0.32 ± 0.05 and 0.18 ± 0.03 mol/column, respectively.

3.2. Equipment

Isocratic experiments were performed using an Ultimate HPLC instrument (LC Packings, San Francisco, CA, USA), with a bypass cartridge supplying flow rates from 200 μl/min to 1.0 ml/min, a 6-port low-dispersion injection valve with a 20 μl sample loop for manual sample injection, and a conventional UZ-view flow cell with 10 μl volume for UV detection. The flow rate in the experiments was controlled at 0.5 ml/min, and the column effluent was monitored at both 280 and 415 nm.

The UZ-view flow cell was connected to a PVDF 50 μl internal volume flow cell matched with a 450CD pH electrode (Sensorex, Garden Grove, CA, USA) so that the pH of the column effluent could be directly measured. To increase the accuracy of the experiments, the directly measured pH of the effluent, not the pH of elution buffer, was used in Eq. (29) when comparing theory and experiments. Digital pH signals were formed within a series network composed of a pH electrode, an Orion 520A pH meter (Orion, Beverly, MA, USA), and a WellChrom interface box V7566 Version 0696. These signals were then relayed through the interface box into the Ultimate instrument, so that pH and UV absorbance data could be collected simultaneously by the computer every 2 s. The pH meter and electrode were calibrated each time before the experiments at a given pH, and the same pH probe was used for measuring both the elution buffer pH and column effluent pH. All the chromatography experiments were controlled by the Ultichrom software version 3.1.

3.3. Procedures

Isocratic experiments were performed in a narrow pH range around the pI value of each protein for both the strong-base and weak-base ion-exchange columns. For each buffer system at a certain fixed pH, the protein was eluted using a series of increasing salt concentrations, which were made by setting different ratios of the two elution buffers A and B. In the case of myoglobin on the Mono

Q column, buffer A was 10 mM triethanolamine, buffer B was 10 mM triethanolamine with 0.5 M NaCl, and both buffers were titrated with 1N HCl to reach the pH values of 8.6, 8.2, 7.7, 7.4 and 7.2 for each series of isocratic experiments. In the case of myoglobin on the Mono P column, buffer A was 10 mM trisma base, buffer B was 10 mM trisma base with 0.5 M NaCl, and both buffers were titrated with 1N HCl to reach the pH values of 8.5, 8.0 and 7.5 for each series of isocratic experiments. In the case of β-lactoglobulin A on the Mono Q column, buffer A was 10 mM 1-methylpiperazine, buffer B was 10 mM 1-methylpiperazine with 0.5 M NaCl, and both buffers were titrated with 1 N HCl to reach the pH values of 5.9, 5.5, 5.2, 4.7, 4.6, and 4.4 for each series of isocratic experiments. In the case of β-lactoglobulin A on the Mono P column, buffer A was 10 mM 1,4-dimethylpiperazine, and buffer B was 10 mM 1,4-dimethylpiperazine with 0.5 M NaCl, and both buffers were titrated with 1N HCl to reach the pH values of 5.2, 5.0, 4.8, 4.7 and 4.5 for each series of isocratic experiments. The columns were presaturated with elution buffer for at least 1 h at 0.5 ml/min at the start of the experiment and each data point was repeated twice.

3.4. Data analysis

Data obtained by the Ultichrom software were transferred to text files and further analyzed in MS Excel. The transit time was taken to be the time for the appearance of the peak maximum. The best fitting values of parameters pI, $(\mathrm{dz/dpH})_{\mathrm{p}I}$, $K_{\mathrm{P,ads}}$, $K_{\mathrm{Cl^-,ads}}$, and $K_{\mathrm{Na^+,ads}}$ were determined by minimizing the sum of the squared residuals between the logarithms of measured k' values and the model calculations. The values of the Donnan potential were calculated numerically as described in Section 2.

4. Fitting experimental results to the multiple charge-state model

4.1. Results using the Mono Q column

Table 1 and Figs. 2 and 3 illustrate the fitting of experimental retention data for myoglobin and β-lactoglobulin A obtained on the Mono Q column to the approximate n charge-state model. To perform the calculations shown for the model, the value of q_{R} given by the column manufacturer of 0.32 mol/cm^3 was assumed. In addition, by determining the retention time t_0 for an unadsorbed eluite, and by assuming $\alpha = 0.4$, the value of ε and q_{R} were determined from Eqs. (32) and (33), with $K_{\mathrm{d,hs}}$ assumed to be zero in the former equation. For the purpose of determining t_0, myoglobin and β-lactoglobulin A were assumed to be unadsorbed at pH 7.2 with 0.5 M NaCl, and at pH 4.4 with 0.5 M NaCl, respectively. Since the value of t_0 was slightly different for the two proteins used, two slightly different values of ε and q_{R} were employed.

Table 1
Comparison of the parameters obtained by fitting experimental isocratic data for myoglobin β-lactoglobulin A on the Mono Q column for several theories

Model	Myoglobin		β-Lactoglobulin A	
	pI	$(\mathrm{dz/dpH})_{\mathrm{p}I}$	pI	$(\mathrm{dz/dpH})_{\mathrm{p}I}$
SD model	6.1	−0.85	3.9	−4.6
Ståhlberg and Jönsson	6.3	−3.1	4.3	−14.7
Sluyterman and Elgersma	8.6	−0.30	5.0	−3.9
Multiple charge-state model	7.7	−1.3	4.9	−9.0
Isoelectric focusing or acid–base titrametry	7.3	−1.6	5.1	−9.8

Parameters for the multiple charge-state model were $\alpha = 0.4$, $K_{\mathrm{Na^+,ads}} = 0$, $K_{\mathrm{Cl^-,ads}} = 1.41/f$, and $q_{\mathrm{R}} = 0.97/f$ and $0.89/f$ mol/l, $\varepsilon = 0.44$ and 0.39, $K_{\mathrm{P,ads}} = 0.055/f$ and $0.118/f$, and $n = 3.4$ and 7.4 for myoglobin and β-lactoglobulin A, respectively. The fitted parameters indicated apply for f ranging from 0.1 to 1.0. The titrametric value of $(\mathrm{dz/dpH})_{\mathrm{p}I}$ for myoglobin was calculated using pK_{a} values for the residue side chains and the terminal amino and carboxyl groups given by Stryer [25]. The other values for pI and $(\mathrm{dz/dpH})_{\mathrm{p}I}$ are experimental results [7,30,31].

An approximate value of f, which is the volume of the adsorbed phase per unit volume of the solid material in the column, was estimated from the maximum adsorption capacity of the Mono Q column for human albumin of 65 mg/ml, as given by the column manufacturer [32]. Using the values of α and ε stated above, and a density of human albumin of 1.25 g/ml, the volume of protein adsorbed under saturation conditions per unit volume of solid material is approximately 0.2, which can also be taken as an approximation for f. However, in fitting the retention data to the model it was determined that only the parameters $K_{\mathrm{P,ads}}$ and $K_{\mathrm{Cl^-,ads}}$ were sensitive to the value of f, while the fitted values of

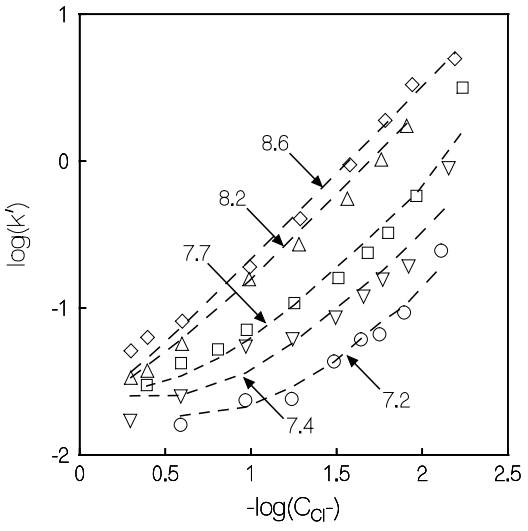

Fig. 2. Plot of the logarithm of the retention factor of myoglobin obtained using a strong-base ion-exchange column packing (Mono Q) vs. the negative logarithm of the concentration of $\mathrm{Cl^-}$. The symbols are data from isocratic experiments, the dashed curves are calculated results from the multiple charge-state model, and the numbers in the figure denote the pH for the calculations. pH 8.6 (◇); pH 8.2 (△); pH 7.7 (□); pH 7.4 (▽); pH 7.2 (○).

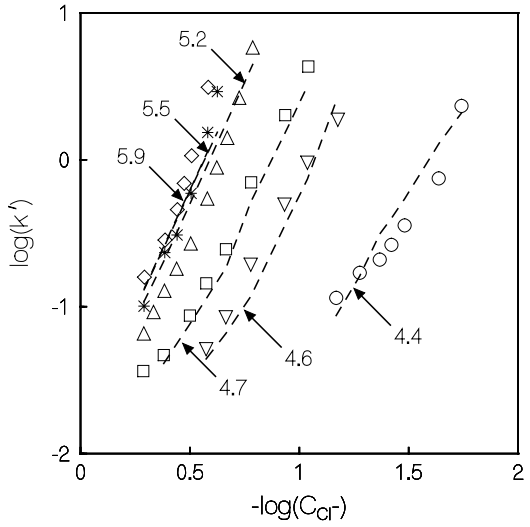

Fig. 3. Plot of the logarithm of the retention factor of β-lactoglobulin A obtained using a strong-base ion-exchange column packing (Mono Q) vs. the negative logarithm of the concentration of Cl^-. The symbols are data from isocratic experiments, the dashed curves are calculated results from the multiple charge-state model, and the numbers in the figure denote the pH for the calculations. pH 5.9 (◇); pH 5.5 (✳); pH 5.2 (△); pH 4.7 (□); pH 4.6 (▽); pH 4.4 (○).

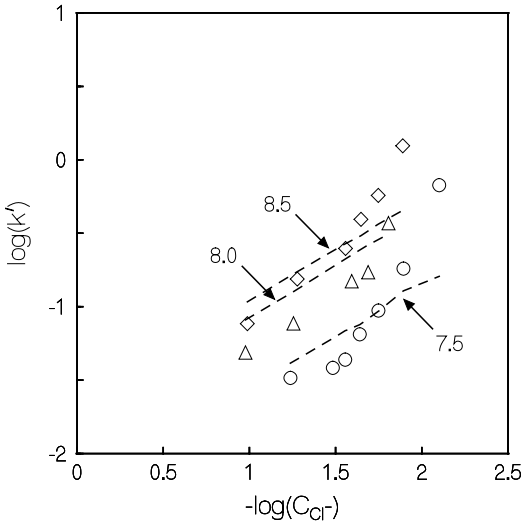

Fig. 4. Plot of the logarithm of the retention factor of myoglobin obtained using a weak-base ion-exchange column packing (Mono P) vs. the negative logarithm of the concentration of Cl^-. The symbols are data from isocratic experiments, the dashed curves are calculated results from the multiple charge-state model, and the numbers in the figure denote the pH for the calculations. pH 8.5 (◇); pH 8.0 (△); pH 7.5 (○).

pI and $(dz/dpH)_{pI}$ were nearly independent of this parameter. Since the fitted values of $K_{P,ads}$ and $K_{Cl^-,ads}$ were also observed to be nearly inversely proportional to f, Table 1 indicates the values of $K_{P,ads}/f$ and $K_{Cl^-,ads}/f$ that apply in the range $0.1 < f < 1.0$.

The fitting of the model to the experimental data was performed by assuming $K_{d,hs}$ to be zero, and then minimizing the sum of the squared errors between the theory and data by adjusting the values of pI, $(dz/dpH)_{pI}$, $K_{P,ads}/f$ and $K_{Cl^-,ads}/f$, and n, while simultaneously solving for the Donnan potential for each data point using Eq. (25) with pK_R set equal to 14 to reflect the fact that Mono Q is a strong-base ion exchanger. It was also assumed that $K_{Cl^-,ads}$ was a property of the column packing, and not of the protein used, so that the same value of this parameter was employed for both myoglobin and β-lactoglobulin A. The data sets for the two proteins were consequently fitted simultaneously to arrive at the single best fitting value of $K_{Cl^-,ads}$. The pH values indicated in Figs. 2 and 3, as well as in Figs. 4 and 5 of the next section, are averages for each data set determined by directly measuring the pH in the column effluent for each individual experiment using the on-line pH flow cell. The actual pH used in Eq. (29) therefore differs slightly from the values indicated in the figures.

Table 1 also illustrates results from using the SD model [6], the model of Ståhlberg and Jönsson [13], and the model of Sluyterman and Elgersma [12] to fit the experimental data. For the former two models, the best straight line was fitted to the data at a particular pH according to the appropriate relation, with the average ionic strength used to determine an average value of B for the Ståhlberg and Jönsson model. In each case the restriction placed on the y intercept by each of the relation used was ignored. Furthermore, since the protein charge at a particular pH determined this way was a nonlinear function of pH, the values of the pI and $(dz/dpH)_{pI}$ were determined by extrapolation to zero charge using a quadratic fit to the data.

As illustrated in Figs. 2 and 3, good agreement was obtained between the experimental data and the calculations

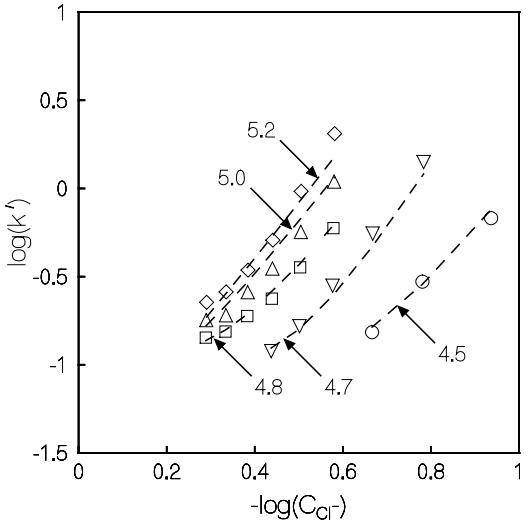

Fig. 5. Plot of the logarithm of the retention factor of β-lactoglobulin A obtained using a weak-base ion-exchange column packing (Mono P) vs. the negative logarithm of the concentration of Cl^-. The symbols are data from isocratic experiments, the dashed curves are calculated results from the multiple charge-state model, and the numbers in the figure denote the pH for the calculations. pH 5.2 (◇); pH 5.0 (△); pH 4.8 (□); pH 4.7 (▽); pH 4.5 (○).

for the multiple charge-state model using the procedures described above. In particular, it can be seen in Fig. 3 that the model is able to accurately predict retention factors for β-lactoglobulin A when the fluid phase pH is below the pI so that the protein in the fluid phase has the same charge sign as the column packing. Although the adsorption of a protein onto a column packing when both have the same charge sign is sometimes cited as evidence of a deficiency in the SD model [19], the results in Fig. 3 suggest that much of the ability of β-lactoglobulin A to adsorb onto an anion exchanger when the fluid phase pH is below the pI can be attributed to the fact that, near the pI, hydrogen ion Donnan equilibrium causes the protein in the fluid and adsorbed phases to have opposite charge signs. Similarly, it can be seen in Fig. 2 that the experimental values of $\log(k')$ plotted against $\log(C_{Cl^-})$ exhibit significant curvature that is well represented by the model. Curvature of this type in experimental data is also sometimes cited as evidence of deficiencies of the SD model, since that model predicts a linear relation between $\log(k')$ and $\log(C_{Cl^-})$ [19].

Another notable trend in Table 1 is that the multiple charge-state model yields values of pI and $(dz/dpH)_{pI}$ that are significantly closer to the values of these parameters determined by isoelectric focusing and acid–base titrametry of the protein in free solution, respectively, as compared to the values of these parameters obtain from the SD, Sluyterman and Elgersma, and Ståhlberg and Jönsson models. The comparatively large error obtained by the Ståhlberg and Jönsson model is not unexpected since this model is unable to account for protein adsorption when the pH is near the protein pI, as discussed earlier. It can also be seen in Table 1 that the relative values of the adsorption constants $K_{P,ads}$ for β-lactoglobulin A and myoglobin are reasonable since, from Eq. (27), this parameter can be interpreted as the adsorption constant for the uncharged form of the protein. The binding of the uncharged form of a protein is likely determined by such factors as the protein hydrophobicity and dipole moment (i.e., charge asymmetry), both of which are higher in value for β-lactoglobulin A than for myoglobin [33,34]. Similarly, the relative values of n and $(dz/dpH)_{pI}$ in Table 1 are reasonable since $(dz/dpH)_{pI}$ is less in absolute value than $-2m^2\ln(10)/3$, and within a factor of two of that expression, which is consistent with the result from the model that $-2\ m^2\ln(10)/3$ is an upper limit for $(dz/dpH)_{pI}$. Finally, it should be noted that in Table 1 and Figs. 2 and 3 that the best fit of the model calculations to the data occurred when Donnan uptake of co-ion into the adsorbed phase was neglected, i.e., when $K_{Na^+,ads} = 0$.

4.2. Results using the Mono P column

Table 2 and Figs. 4 and 5 illustrate the fitting of experimental retention data for myoglobin and β-lactoglobulin A obtained on the Mono P column to the multiple charge-state model. The calculations shown were performed as described above for the Mono Q column except that a value of 9.0 for pK_R was assumed in Eq. (25) to approximate the titration behavior of the Mono P column, which is reported to incorporate a mixture of quaternary and tertiary amine functional groups [32]. Since this crude representation resulted in considerably more uncertainty in determining the charge density on the column packing, and therefore more uncertainty in the Donnan potential, for the Mono P column as compared to the Mono Q column, the data fitting procedure was simplified by assuming that the values of m for the two proteins were independent of the column packing used. The values of these parameters obtained on the Mono Q column were consequently used for the Mono P column and were not further adjusted. During the data fitting procedure it was again observed that the chosen value of the parameter f mainly affect the fitted values of $K_{P,ads}$ and $K_{Cl^-,ads}$, and that the latter two parameters were nearly inversely proportional to the chosen value of f. Table 2 therefore again reports the values of $K_{P,ads}/f$ and $K_{Cl^-,ads}/f$ that apply in the range $0.1 < f < 1.0$.

Table 2
Comparison of the parameters obtained by fitting experimental isocratic data for myoglobin and β-lactoglobulin A on the Mono P column to the multiple charge-state model

Model	Myoglobin		β-Lactoglobulin A	
	pI	$(dz/dpH)_{pI}$	pI	$(dz/dpH)_{pI}$
Multiple charge-state model	7.9	−1.77	4.7	−6.6

Parameters for the multiple charge-state model were $\alpha = 0.4$, $K_{Na^+,ads} = 0$, $K_{Cl^-,ads} = 1.07/f$, and $q_R = 0.78/f$ and $0.64/f$ mol/l, $\varepsilon = 0.52$ and 0.61, $K_{P,ads} = 0.103/f$ and $0.295/f$, and $n = 3.4$ and 7.4 for myoglobin and β-lactoglobulin A, respectively. The fitted parameters indicated apply for f ranging from 0.1 to 1.0.

Table 2 and Figs. 4 and 5 indicated that the multiple charge-state model is able to fit experimental data obtained on the Mono P column utilizing values of pI and $(dz/dpH)_{pI}$ that are reasonably close to the values of these parameters obtained in Table 1 for the Mono Q column. Many of the other trends apparent in Table 2 and Figs. 4 and 5 are also similar to those observed for the Mono Q column. For example, it can again be seen for the particular case of β-lactoglobulin A that the model accurately predicts the retention factors when the fluid phase pH is below the protein pI so that the protein in the fluid phase has the same charge sign as the column packing, and that the curvatures of the data and model calculations approximately agree. In general, however, the agreement between the data and the model calculations is less for the Mono P column as compared to the Mono Q column, likely because of the higher uncertainty in determining the Donnan potential for the former column as discussed above. In addition, it can be seen that the value of $K_{P,ads}$ obtained on the Mono P column is greater for β-lactoglobulin A than for myoglobin, which again likely reflects the greater hydrophobicity and dipole moment of the former protein. Finally, it can be seen that the values of $K_{P,ads}$ for the two proteins are greater on the Mono P column as compared to the Mono Q column, which likely reflects the fact that the former column is composed

Table 3
Properties of three proteins determined from isocratic retention data and the multiple charge-state model, or reported in the literature as denoted by the references indicated

Protein	Isoelectric focusing	Acid–base titrametry	Multiple charge-state model				
	pI	$(dz/dpH)_{pI}$	pI	$(dz/dpH)_{pI}$	n	$K_{P,ads}$	$K_{Cl^-,ads}$
Albumin (human serum)	5.8 [8]	−10.0 [35]	5.6	−8.1	11.6	0.46	4.0
β-Lactoglobulin A (bovine milk)	5.1 [30]	−9.8 [31]	5.1	−9.7	8.7	0.82	2.3
Ovalbumin (egg white)	4.7 [30]	−8.9 [36]	5.2	−5.2	10.9	1.11	5.1

Calculations assume there is no Donnan uptake of co-ion.

of polyethyleneimine, which is a relatively hydrophobic polymer.

4.3. Additional results from previous work

The approximate n charge-state model was further evaluated using three sets of data from isocratic experiments published in the literature as summarized in Table 3. In the first data set, retention factors for human serum albumin were obtained using a Mono Q column at the pH values of 5.5 and 6.5 with various ionic strengths [8]. Using the same values of q_R, α and ε as used for the Mono Q column in Table 1, the multiple charge-state model was able to fit the experimental data reasonably well as shown in Fig. 6. Furthermore, as shown in Table 3, the fitted values of pI and $(dz/dpH)_{pI}$ are in reasonable agreement with these values determined by isoelectric focusing and acid–base titrametry of the protein in free solution, respectively. In the second data set, retention factors for β-lactoglobulin A were obtained using a SynChropack AX 300 column in the fully quaternized form at the pH values of 5.0 and 6.0 with various ionic strengths [7]. Since values for q_R, α, and ε for this column were not available, these values were assumed to be the same as for the Mono Q column described in Table 1. The results from fitting the data to the multiple charge-state model is shown in Fig. 7 where it can be seen that the data and theory are in good agreement. In addition, the fitted values for pI and $(dz/dpH)_{pI}$ are consistent with the values obtained for β-lactoglobulin A from the Mono Q column as discussed in the previous section. For the third data set, retention factors for ovalbumin were obtained using a SynChropack Q 300 column at the pH values of 5.0 and 6.0 with various ionic strengths [19]. Since SynChropak Q 300 is a strong-base ion-exchange column packing, and because the physical properties were again not available, the values of q_R, α and ε were also assumed to be the same as for the Mono Q column. A comparison of the experimental data and calculations from the multiple charge-state model is shown in Fig. 8, where again it can be seen that the agreement is reasonably good. Furthermore, the fitted values of pI and $(dz/dpH)_{pI}$ can be

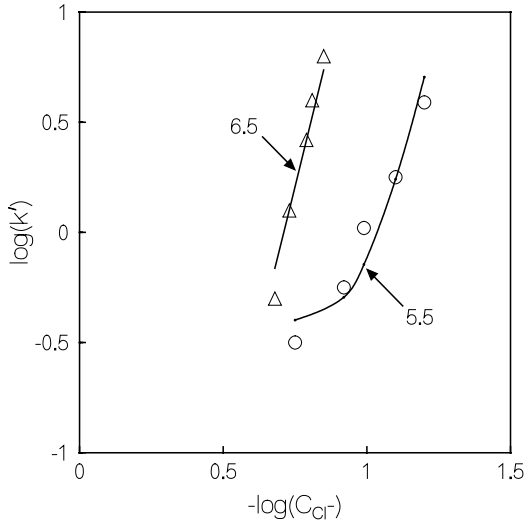

Fig. 6. Plot of the logarithm of the retention factor of albumin using a strong-base ion-exchange column packing (Mono Q) vs. the negative logarithm of the concentration of Cl^- obtained. The symbols are data from isocratic experiments, the solid curves are calculated results from the multiple charge-state model, and the numbers in the figure denote the pH for the calculations. In the experiments the fluid phase contained 20 mM piperazine and 20 mM bis–tris at pH 5.5 and 6.5, respectively, with various amounts of NaCl added, and the flow rate was 1.0 ml/min. pH 6.5 (△); pH 5.5 (○).

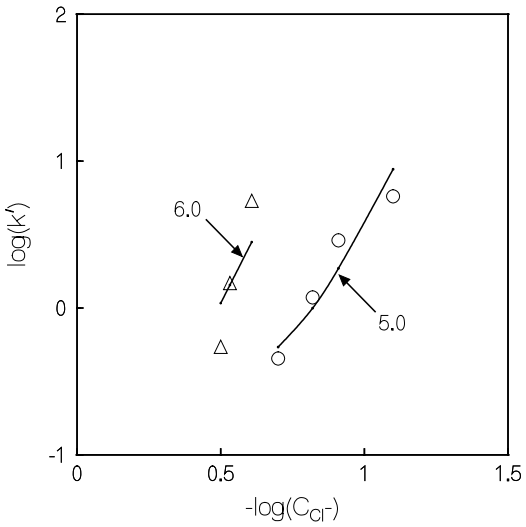

Fig. 7. Plot of the logarithm of the retention factor of β-lactoglobulin A obtained using a strong-base ion-exchange column packing (SynChropak AX 300, manufactured by SynChrom) vs. the negative logarithm of the concentration of Cl^-. The symbols are data from isocratic experiments, the solid curves are calculated results from the multiple charge-state model, and the numbers in the figure denote the pH for the calculations. pH 6.0 (△); pH 5.0 (○).

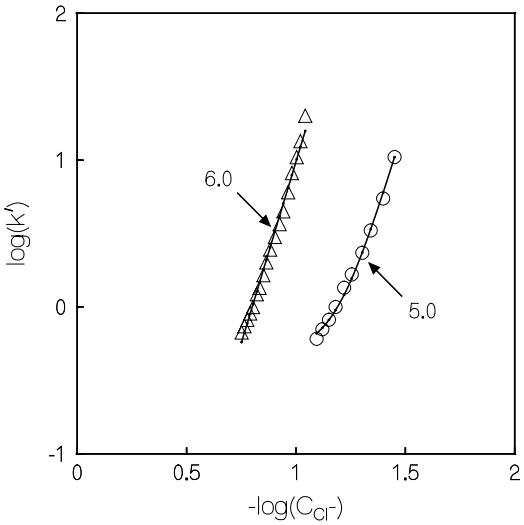

Fig. 8. Plot of the logarithm of the retention factor of ovalbumin obtained using a strong-base ion-exchange column packing (SynChropak Q 300 manufactured by SynChrom) vs. the negative logarithm of the concentration of Cl^-. The symbols are data from isocratic experiments, the solid curves are calculated results from the multiple charge-state model, the numbers in the figure denote the pH for the calculations, and the symbols represent the pH. pH 6.0 (△); pH 5.0 (○). In the experiments, the fluid phases contained 20 mM piperazine at pH 5.0 and 6.0 with various amount of NaCl added, and the flow rate was 0.5 ml/min.

seen in Table 3 to again be in reasonable agreement to the results obtained from isoelectric focusing and acid–base titration of the protein in free solution, respectively.

5. Discussion and conclusions

The stoichiometric displacement model for protein ion-exchange adsorption equilibrium was introduced by Boardman and Partridge [6] nearly one-half century ago, and is widely used even today to fit protein adsorption equilibrium data. Despite its widespread use, the SD model ignores certain phenomena generally thought to be important in determining the ion-exchange equilibrium of proteins, such as the diffuse nature of the electrical double layer adjacent to the adsorbent surface, the asymmetric charge distribution on the protein, aggregation and unfolding of the protein, and protein charge regulation, i.e., the change in protein charge caused by electrostatic effects during adsorption. Although a number of more recent studies have made progress in accounting for many of these aspects [7–11,21], only the work of Sluyterman and Elgersma [12] and Ståhlberg and Jönsson [13] appear to address quantitatively the effects of protein charge regulation.

In the present study, a new model is developed which accounts for protein charge regulation during the ion-exchange adsorption of a dilute protein more accurately than either the Sluyterman and Elgersma [12] or Ståhlberg and Jönsson [13] models, particularly for the case of most interest where the fluid phase pH is near the protein p*I*. In the new model, protein charge regulation is accounted for by representing the adsorbed phase as being uniform in composition, and then including the effects of hydrogen ion Donnan equilibrium more realistically than in the original Sluyterman and Elgersma model so that an improved theoretical description results for protein ion-exchange equilibrium. The new model can also be considered an extension of the SD model since, when the fluid phase pH is far from the protein p*I*, the protein charge in the new model becomes identical to the "characteristic binding charge" of the SD model.

Experimental results for the case where the fluid phase pH is near the protein p*I* for four proteins obtained on four different column packings indicate that the new model, as represented by Eq. (29), is able to fit experimental adsorption data with the values of p*I* and $(dz/dpH)_{pI}$ used in that equation more nearly equal to the values of these parameters obtained from isoelectric focusing and acid–base titrametry of the protein in free solution, respectively, as compared to the values of these parameters obtained by determining the characteristic charge from the SD model as a function of pH. Consequently, the results indicate that when the pH is near the protein p*I*, protein charge regulation is an important factor which causes a discrepancy between the characteristic binding charge from the SD model and the electrical charge on the protein in free solution. When the pH is far from p*I* the situation is likely even more complicated since the higher charge on the protein, and possibly its higher charge asymmetry, may cause additional deviations from the ideal behavior assumed in the development of the SD model. However, this region was not considered here since Eq. (29) assumes the existence of just three charge states and therefore cannot be applied accurately over a broad pH range.

Although the results obtained in this study cannot be considered a complete validation of the accuracy of Eq. (29) for describing protein ion-exchange equilibrium when the pH is near the protein p*I*, they do suggest that this equation is a useful improvement over the traditional SD model. Furthermore, since operation at a pH near the p*I* has been reported as a means to improve the resolution of proteins when using ion-exchange chromatography with salt gradient elution, and since elution at a pH near the protein p*I* is necessary characteristic of ion-exchange chromatography using a pH gradient, it is also likely that Eq. (29) has practical uses in the design and optimization of chromatographic processes for protein purification. In addition, Eq. (29) is a useful means for providing a characteristic binding charge corrected for protein charge regulation so that other phenomena not accounted for by the SD model, such as protein unfolding during adsorption, can be more easily identified. Finally, due to its reliance on rigorous thermodynamic principles, Eq. (29) provides a relatively simple formalism for incorporating the effect of hydrogen ion Donnan equilibrium on the protein charge into recently developed molecular thermodynamic approaches that describe the partitioning of a protein between two aqueous phases [23], or between an aqueous phase and a charged hydrogel [24].

6. Nomenclature

a_{H^+}	activity of the hydrogen ion
A_P	total surface area of a spherical protein (m^2/molecule)
A_P^0	protein surface area interacting with the column packing ($A_P^0 = 1/2A_P$) (m^2/molecule)
B	constant in Eq. (6)
C_{Cl^-}	concentration of Cl^- in the fluid phase (mol/l)
C_{H^+}	concentration of H^+ in the fluid phase (mol/l)
C_P	concentration of all protein forms in the fluid phase (mol/l)
C_{Na^+}	concentration of Na^+ in the fluid phase (mol/l)
C_{Pi}	concentration of protein form i in the fluid phase, where $i = m$, 0, or $-m$ (mol/l)
D	diameter of column (cm)
f	fraction of the entire solid material constituting the adsorbed phase
F	Faraday's constant (C/mol)
G	Gibbs free energy (J/mol)
I	ionic strength (mol/l)
k'	retention factor
K_B	constant in Eq. (1)
$K_{Cl^-,ads}$	adsorption equilibrium constant for Cl^-
K_d	distribution coefficient
$K_{d,hs}$	distribution coefficient at high salt conditions
$K_{Na^+,ads}$	adsorption equilibrium constant for Na^+
$K_{Pi,ads}$	adsorption equilibrium constant for protein form i, where $i = m$, 0, or $-m$
$K_{P,1}$, $K_{P,2}$	dissociation constants in the multiple charge-state model
K_R	dissociation constant for the functional group on the column packing
K_1, K_2	dissociation constants in the Sluyterman and Elgersma model
L	length of column (cm)
m	parameter used in the approximate n charge-state model, where $n = 2m + 1$
n	total number of charge states for a protein that exist between the m and $-m$ charge states
P	phase ratio
pI	isoelectric point of a protein
pI'	pH where the distribution coefficient equals unity
pI_{app}	apparent pI observed in chromatofocusing
q_{Cl^-}	concentration of Cl^- in the adsorbed phase (mol/l)
q_{H^+}	concentration of H^+ in the adsorbed phase (mol/l)
q_{Na^+}	concentration of Na^+ in the adsorbed phase (mol/l)
q_P	concentration of all protein forms in the adsorbed phase (mol/l)
q_{Pi}	concentration of protein form i in the adsorbed phase, where $i = m$, 0, or $-m$ (mol/l)
q_R	concentration of the functional group R in the adsorbed phase (mol/l)
q_{R^+}	concentration of the charged form of the functional group R in the adsorbed phase (mol/l)
$q_{R,col}$	quantity of the functional group R per unit volume of column (mol/column)
R	ideal gas constant (J/mol K)
t	transit time of an eluite (s)
t_D	the time associated with the extra-column volume (s)
t_M	transit time under high salt conditions (s)
t_0	transit time of an unretained eluite corrected for the extra-column volume, $t_0 = t_M - t_D$ (s)
T	absolute temperature (K)
v_{fluid}	linear (i.e., interstitial) fluid velocity (cm/s)
z	protein charge

Greek letters

α	interparticle void volume of the column
γ_{H^+}	activity coefficient of H^+
ε	intraparticle void volume (particle porosity)
ε_r	dielectric constant of medium
ε_0	permittivity of free space (C/V m)
κ	inverse Debye length (m^{-1})
σ_P	charge density on the protein surface is in the bulk fluid (C/m^2)
ϕ	dimensionless Donnan potential, equivalent to $\ln(C_{H^+}/q_{H^+})$
ψ_s	surface potential

Superscript

$*$	equilibrium value

Acknowledgements

Support from grant CTS 9813658 from the National Science Foundation is greatly appreciated.

References

[1] S.H. Behrens, M. Borkovec, J. Chem. Phys. 111 (1999) 382.
[2] D. Chan, J.W. Perram, L.R. White, T.W. Healy, J. Chem. Soc., Faraday Trans. I 71 (1975) 1046.
[3] S.L. Carnie, D.Y. Chan, J.S. Gunning, Langmuir 10 (1994) 2993.
[4] S.H. Behrens, D.G. Grier, J. Chem. Phys. 115 (2001) 6716.
[5] B.W. Ninham, V.A. Parsegian, J. Theor. Biol. 31 (1971) 405.
[6] N.K. Boardman, S.M. Partridge, Biochem. J. 59 (1955) 543.
[7] W. Kopaciewicz, M.A. Rounds, J. Fausnaugh, F.E. Regnier, J. Chromatogr. 266 (1983) 3.
[8] M.T.W. Hearn, A.N. Hodder, P.G. Stanton, M.I. Aguilar, Chromatographia 24 (1987) 769.
[9] C.M. Roth, K.K. Unger, A.M. Lenhoff, J. Chromatogr. A 726 (1996) 45.
[10] J. Ståhlberg, B. Jönsson, Cs. Horváth, Anal. Chem. 63 (1991) 1867.

[11] W.R. Melander, Z.E. Rassi, Cs. Horváth, J. Chromatogr. 469 (1989) 3.
[12] L.A.A. Sluyterman, O. Elgersma, J. Chromatogr. 150 (1978) 17.
[13] J. Ståhlberg, B. Jönsson, Anal. Chem. 68 (1996) 1536.
[14] L.A.A. Sluyterman, J. Wijdenes, J. Chromatogr. 150 (1978) 31.
[15] R.K. Scopes, Protein Purification: Principles and Practice, Springer-Verlag, New York, 1987.
[16] S. Yamamoto, T. Ishihara, J. Chromatogr. A 852 (1999).
[17] J.T.G. Overbeek, Prog. Biophysics Biophys. Chem. 6 (1956) 57.
[18] M.A. Rounds, F.E. Regnier, J. Chromatogr. 283 (1984) 37.
[19] I. Mazsaroff, L. Vàrady, G.A. Mouchawar, F.E. Regnier, J. Chromatogr. 499 (1990) 63.
[20] P. DePhillips, A.M. Lenhoff, J. Chromatogr. A 933 (2001) 57.
[21] J.C. Bosma, J.A. Wesselingh, AIChE J. 44 (1998) 2399.
[22] P.-A. Albertsson, Partition of Cell Particles and Macromolecules, Wiley Interscience, New York, 1986.
[23] C.A. Haynes, J. Carson, H.W. Blanch, J.M. Prausnitz, AIChE J. 37 (1991) 1401.
[24] A.P. Sassi, H.W. Blanch, J.M. Prausnitz, AIChE J. 42 (1996) 2335.
[25] L. Stryer, Biochemistry, Freeman, San Francisco, 1975.
[26] G.E. Clement, A. Siegel, R. Potter, Can. J. Biochem. 49 (1971) 477.
[27] J.S. Newman, Electrochemical Systems, Prentice-Hall, Englewood Cliffs, NJ, 1973.
[28] J.C. Strong, D.D. Frey, J. Chromatogr. A 769 (1997) 129.
[29] J.C. Giddings, Unified Separation Science, Wiley, New York, 1991.
[30] P.G. Righetti, T. Caravaggio, J. Chromatogr. 127 (1976) 1.
[31] R.K. Cannan, A.H. Palmer, A.C. Kibrick, J. Biol. Chem. 142 (1942) 803.
[32] Biodirectory'99 Product Catalog, Amersham Pharmacia Biotech, Uppsala, 1999.
[33] V.P. Shanbhag, C.-G. Axelsson, Eur. J. Biochem. 60 (1975) 17.
[34] X. Kang, D.D. Frey, J. Chromatogr. A 991 (2003) 117.
[35] C. Tanford, J. Am. Chem. Soc. 72 (1950) 441.
[36] R.K. Cannan, A. Kibrick, A.H. Palmer, Ann. N. Y. Acad. Sci. 41 (1941) 243.